Available online at www.sciencedirect.com
SCIENCE DIRECT
Journal of Power Sources 153 (2006) 350–353
JOURNAL OF POWER SOURCES
www.elsevier.com/locate/jpowsour

Short communication

Nanoparticled $Li(Ni_{1/3}Co_{1/3}Mn_{1/3})O_2$ as cathode material for high-rate lithium-ion batteries

Shichao Zhang [a,*], Xinping Qiu [b], Zhiqi He [b], Dangsheng Weng [a], Wentao Zhu [b]

[a] *School of Material Science and Engineering, Beihang University, Beijing 100083, PR China*
[b] *Key Lab of Organic Optoelectronics and Molecular Engineering, Department of Chemistry, Tsinghua University, Beijing, 100084, China*

Available online 19 July 2005

Abstract

Nanoparticle of $Li(Ni_{1/3}Co_{1/3}Mn_{1/3})O_2$ with size smaller than 40 nm was obtained by non-aqueous system co-precipitation method. The particle morphology and crystal plane orientation were observed by TEM and HRTEM. Electrochemical properties of this nanostructued material were studied with experiment cells. The results show that the material has high capacity of 160 mAh g^{-1} and excellent rate capability for charge and discharge. For the 50C and 100C rate, its capacity remains above 100 mAh g^{-1} after tens of cycles.

Keywords: Lithium-ion battery; Cathode; Nanoparticle; Rate capability

1. Introduction

Lithium-ion batteries (LIBs) have long been considered as possible power source for electric vehicle (EV) and hybrid electric vehicle (HEV) [1] for their high power density and long cycle life. However, two main problems concerning the use of LIBs in EV or HEV should be solved: high-rate performance and safety. Comparing with anode materials and electrolytes, cathode materials with good rate performance now seem to be the bottleneck and have attracted much attention. It was reported that thin-film [2] and highly porous [3] positive electrodes could improve the charge/discharge rate of LIBs. However, as far as we know, few experiments for LIBs cycled at a rate as high as 10C or more were done. Using nanostructured cathode materials seems to be another promising solution to the problem [4,5]. However, it is very hard to obtain nanosized lithium complex metal oxides smaller than 100 nm.

$LiCoO_2$ has been widely used in commercial LIBs for more than 10 years. Recently, many kinds of cathode materials such as $LiNiO_2$ [6], $LiMn_2O_4$ [7], $LiMnO_2$ [8] and $LiFePO_4$ [9] were synthesized and reported, in which low cost and abundant elements, such as Mn and Ni, were used to substitute expensive and toxic Co. $Li(Ni_{1/3}Co_{1/3}Mn_{1/3})O_2$ was reported recently and showed large capacity and good cycle performance [10–12]. Here, we report our work of synthesis of $Li(Ni_{1/3}Co_{1/3}Mn_{1/3})O_2$ nanoparticle smaller than 40 nm for cathode material of LIBs by non-aqueous system co-precipitation method. This nanostructured material exhibits good cyclability at rate as high as 100C, very useful for the development of "green" vehicles.

2. Experimental

Nanosized $Li(Ni_{1/3}Co_{1/3}Mn_{1/3})O_2$ samples were prepared by chemical co-precipitation method in similar to reported [4]. $LiNO_3$, $Ni(NO_3)_2$, $Co(NO_3)_2$ and $MnCl_2$ as the starting materials were dissolved in ethanol with the mole ratio of 3.3:1:1:1, and the total concentration of the solution is 3 M. The solution was dropped into the strongly stirred 3 M KOH/ethanol solution with a speed of one drop per second. Precipitate was separated from the solution and dried at 80 °C for 10 h. Finally, the primary samples were calcined in a temperature range from 400 to 800 °C.

The calcined samples were stirred with 30 wt% acetylene black and 10 wt% PVDF in NMP solvent to make electrodes.

* Corresponding author. Tel.: +86 10 82338148; fax: +86 10 82316100.
E-mail address: csc@buaa.edu.cn (S. Zhang).

0378-7753/$ – see front matter © 2005 Published by Elsevier B.V.
doi:10.1016/j.jpowsour.2005.05.021

The electrochemical performance was evaluated with experimental cells using a metallic Li foil as anode and 1 M $LiPF_6$ in 50–50% EC/DMC as the electrolyte. Galvanostatic experiments were performed with an electrochemistry interface (Solartron 1287).

3. Results and discussion

TGA (TGA 2050, TA) measurement of the precipitates showed that the reaction began at 300 °C and mass reduction ended at about 385 °C. They were calcined in various temperatures to prepare different samples. Samples A–D were prepared at 400, 500, 600 and 700 °C for 6 h, respectively, and sample E was prepared at 600 °C for 6 h and then 800 °C for 2.5 h. ICP (OPTIMA 3300RL) was employed to measure the final elements ratio in the samples. The atom ratio of Li:Ni:Co:Mn in the sample E is equal to 1.05:0.33:0.33:0.33, where the atom ratio of the transition metals is equal to that of starting materials. XPS (PHI-5300, ESCA) was used to investigate the valence of the elements in the material. It shows that Mn mostly appears +4 valence, Ni mostly appears +2 valence and Co mostly appears +3 valence. This result matches well with the XPS results obtained by Shaju et al. [11].

Fig. 1 shows the powder X-ray powder diffraction (D/MAX-RB) patterns of samples calcined at various temperatures. It indicates that the samples have good rock-salt structure without any impure phase. Obvious peak expansion shows that the material has very fine grain. We used formula of Scherrer to calculate the grain size of each samples. Grain size of samples A–E are 5.4, 8.0, 14.9, 28.0 and 42.0 nm, respectively. It has been reported by Lu and Dahn [10,12] and Shaju et al. [11] that the peak intensity ratio R of (0 0 3)/(1 0 4) of $Li(Ni_xCo_{(1-2x)}Mn_x)O_2$ was not so high with $x = 1/4$, 1/3 and 3/8. It means the cation mixing of Li^+ and Ni^+ [10] and it is well known to be an important reason for capacity fading. However, $Li(Ni_{1/3}Co_{1/3}Mn_{1/3})O_2$ prepared by this co-precipitation method shows very high R value. It can be found in Fig. 1 that R is larger than 1.0 when synthesis temperature is above 600 °C. When the sample prepared at 600 °C was recalcined at 800 °C for 2.5 h after washing and drying, R increased from 1.09 to 2.28 and the peak splitting of (0 0 6), (1 0 2) pair and (0 1 8), (1 1 0) pair could been found clearly. This means that sample E has ideal rock-salt layered structure and the cation mixing is largely restrained.

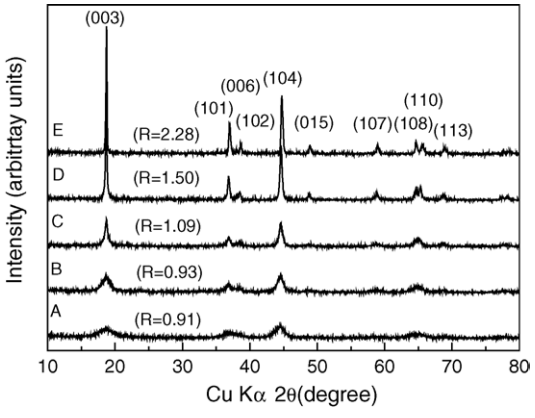

Fig. 1. X-ray powder diffraction patterns for samples A–E. A–D are prepared at 400, 500, 600 and 700 °C for 6 h, respectively. Sample E is prepared at 600 °C for 6 h and then 800 °C for 2.5 h.

Fig. 2a is the TEM (JEOL JEM-CX100) picture of the particle of the sample E. The particle has uniform size with a narrow size distribution. The particle size is in the range of 10–40 nm. The electron diffraction pattern as shown in Fig. 2b indicates that the particle is well crystallized. HRTEM (JEOL JEM-2010) was also employed to study the morphology of the particle. There are three kinds of typical particles as shown in Fig. 2c–e. Among the three types of particles, it can be observed from Fig. 2a that rectangle shaped particle as shown in Fig. 2c is predominant. Most of this kind of particle is single crystal. The interplanar distance of the grain in Fig. 2c is about 0.47 nm, which is approx to the interplanar distance of (0 0 3) plane (0.475 nm, calculated from XRD pattern). It indicates that (0 0 3) planes are vertical to the surface of the particle. Obviously, it is favorable for lithium ion intercalation from electrolyte into 2D channels between (0 0 3) planes of the particle [13]. In Fig. 2d, the single crystal particle has a different interplanar distance of layers, which is about 0.20 nm. It can be assigned to (1 0 4) plane (0.203 nm, calculated from XRD pattern). Another kind of particle is multicrystalline like the one shown in Fig. 2e. Most of them have the first kind of interplanar distance and also a few have the second kind of interplanar distance.

The charge and discharge curves from the first to the10th recorded with 0.2 mA cm^{-2}, corresponding to a 1C rate, are shown in Fig. 3. The first charge and discharge capacity are, respectively, 180 and 160 mAh g^{-1} between 4.25 and 2.5 V. The discharge profile shows a long slope line between 3.5 and 2.5 V. It was explained to be according to the capacity of amorphous phase in the cathode material [15]. However, we suggest that this capacity is due to the surface part of the fine particle because amorphous phase is not observed in our samples.

The discharge capacities of sample E at various rates are shown in Fig. 4. Commercial $LiCoO_2$ with a particle size of 2–8 μm is used for a comparison. The contents of acetylene and PVDF in the electrodes are the same. The upper cut off voltage is controlled in the range of 4.3–4.7 V and the lower cut off voltage is 2.5–1 V, according to the charge–discharge rate used. Fig. 4 shows that the commercial $LiCoO_2$ also exhibits high capacity at the first cycle at 50C rate because acetylene black content is high enough. However, its capacity fades quickly in the first several cycles. It may be due to that the surface of $LiCoO_2$ particle is overcharged at the high current density, while Li ions in bulk lattice cannot diffuse or transfer to the surface in time because of a long diffusion path. In this case, the layer structure of the surface of the particle is irreversibly destroyed and the capacity faded [14]. For the

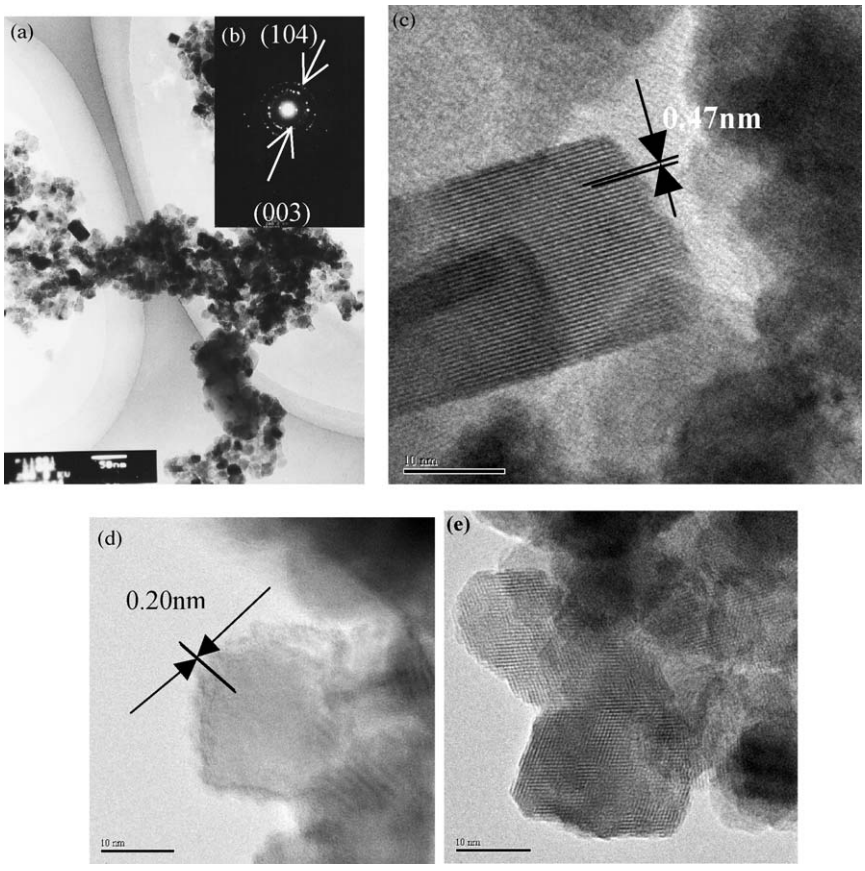

Fig. 2. (a) Transmission electron micrograph of sample E. The bar is 50 nm. (b) Electron diffraction pattern. (c–e) HRTEM pictures of the particles. The bars are all 10 nm.

nanoparticled material, however, it has many advantages for fast charge and discharge. The area of the interface between the electrolyte and the active material is very large and the diffusion path of lithium ion from bulk to surface is very short. On the other hand, as mentioned above, most of the particles have a good orientation that (0 0 3) planes are vertical to the surface. In Fig. 4, sample E shows excellent capacity at high charge and discharge rates. For 10C, 50C and 100C rate (if 100 mAh g^{-1} is used as the average capacity), the discharge

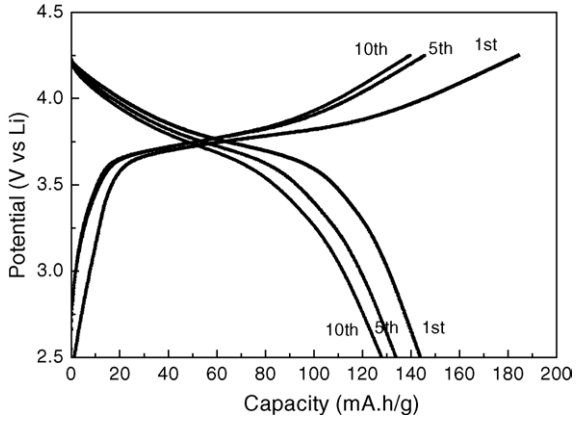

Fig. 3. The charge and discharge curves from the first to the10th cycles of the cell Li/Li($Ni_{1/3}Co_{1/3}Mn_{1/3}$)O_2 with current density of 0.2 mA cm^{-2}, corresponding to a 1C rate.

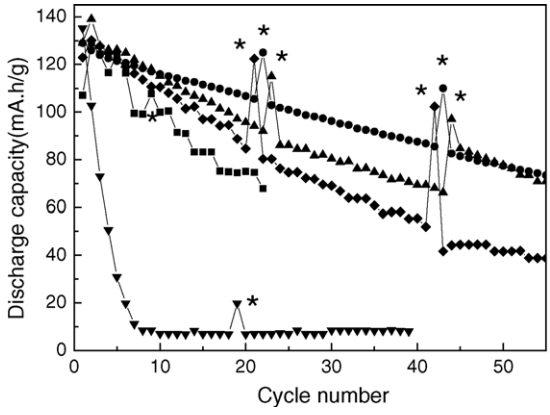

Fig. 4. Cycle capacity at various current densities of sample E (calcined at 600 °C for 6 h and 800 °C for 2.5 h) and commercial $LiCoO_2$, (●), sample E, 1000 mA g^{-1}, 2.5–4.3 V; (▲), sample E, 5000 mA g^{-1}, 1.5–4.35 V (1–4.35 V for 45–55 cycle); (♦), sample E, 10,000 mA g^{-1}, 1.5–4.5 V; (■), sample E, 30,000 mA g^{-1}, 1–4.7 V; (▼), $LiCoO_2$, 5000 mA g^{-1}, 1.5–4.7 V; (⋆), 100 mA g^{-1}, 2.5–4.25 V.

capacity of the first cycle is 129, 129 and 123 mAh g^{-1}, respectively. After 30 cycles, the remaining percentage of the capacity is 74, 61 and 54%, respectively. For 300C rate, corresponding to a current density of about 25 mA cm^{-2}, the discharge capacity of the first cycle is 107 mAh g^{-1}, and after 20 cycles 70% of the capacity remains. If we use low rate of 1C after a number of high-rate cycles, as shown in Fig. 4, the capacity of the material can recover from 79 to 95% of the maximum capacity while commercial $LiCoO_2$ cannot. The results indicate that the material has a good reversibility, and the capacity fading at high charge and discharge rate may be due to the IR polarization caused by the low conductivity of the electrolyte.

4. Conclusions

The cathode material of $Li(Ni_{1/3}Co_{1/3}Mn_{1/3})O_2$ with the particle size of 10–40 nm shows excellent performance at high charge and discharge rates. The small particle size and good (0 0 3) plane orientation are the important factors for the fast Li^+ intercalation and de-intercalation properties. It means that LIBs may be fully charged or discharged within 0.5 s and cycled well by using nanostructured cathode materials. Hence, the power density of LIBs may be enhanced to 15,000 kW kg^{-1}, well meeting the requirement of "green" vehicles such as EV and HEV. Also, it is very helpful to reducing the charge time of batteries in portable electric devices.

Acknowledgement

This work is supported by the Special Funds for Major State Basic Research Project of China (2002CB211800).

References

[1] I.B. Weinstock, J. Power Sources 110 (11) (2002) 471–474.
[2] J.B. Bates, N.J. Dudney, B. Neudecker, A. Ueda, C.D. Evans, Solid State Ionics 135 (1–4) (2000) 33–45.
[3] K.M. Abraham, D.M. Pasquariello, E.M. Willstaedt, J. Electrochem. Soc. 145 (2) (1998) 482–486.
[4] H.L. Chen, X.P. Qiu, W.T. Zhu, P. Hagenmuller, Electrochem. Commun. 4 (6) (2002) 488–491.
[5] J.M. Tarascon, M. Mrmand, Nature 414 (2001) 359–367.
[6] R. Kanno, H. Kubo, Y. Kawamoto, T. Kamiyama, T. Izumif, Y. Takeda, M.J. Takano, Solid State Chem. 110 (2) (1994) 216–225.
[7] R.J. Gummow, A. Dekock, M.M. Thackeray, Solid State Ionics 69 (1) (1994) 59–67.
[8] A.R. Armstrong, P.G. Bruce, Nature 381 (6582) (1996) 499–500.
[9] A.K. Padhi, K.S. Nanjundaswamy, J.B. Goodenough, J. Electrochem. Soc. 144 (4) (1997) 1188–1194.
[10] Z.H. Lu, J.R. Dahn, J. Electrochem. Soc. 148 (3) (2001) A237–A240.
[11] K.M. Shaju, G.V.S. Rao, B.V.R. Chowdari, Electrochim. Acta 48 (2002) 145–151.
[12] D.D. MacNeil, Z.H. Lu, J.R. Dahn, J. Electrochem. Soc. 149 (10) (2002) A1332–A1336.
[13] J.B. Bates, N.J. Dudney, B.J. Neudecker, F.X. Hart, H.P. Jun, S.A. Hackney, J. Electrochem. Soc. 147 (1) (2000) 59–70.
[14] Z.X. Wang, X.J. Huang, L.Q. Chen, J. Electrochem. Soc. 150 (2) (2003) A199–A208.
[15] J. Kim, A. Manthiram, Nature 390 (1997) 265–267.